International Research Journal of Engineering and Technology (IRJET) e-ISSN: 2395-0056
Volume: 07 Issue: 07 | July 2020 www.irjet.net p-ISSN: 2395-0072

Parametric Optimization of Gas Tungsten ARC Welding for Austenitic Stainless Steel J4 and Brass C21000 using Taguchi Design

Savyasachi N[1], Geo Sebastian[2], Jain Anna Sajan[3]

[1]Assistant Professor, Department of Metallurgical and Materials Engineering, Amal Jyothi College of Engineering, Kanjirappally, India
[2]Student, University of Windsor, 401 Sunset Ave, Windsor, Ontario, N9B3P4
[3]Student, Department of Metallurgical and Materials Engineering, Amal Jyothi College of Engineering, Kanjirappally, India

---

Abstract - *Welding of Stainless Steel and Copper alloys is an important issue because of their increasing applications. The combination of stainless steel and copper alloys is found in pressure vessels, boilers, and other high temperature components. When stainless steel alloys are used at high temperatures, heat dissipation to the environment is low because of their low thermal conductivity.*

This work focusses on joining of Austenitic stainless steel J4 and Brass C21000. A sound weld between these was performed by Gas Tungsten Arc Welding using Silver 40 filler material. The parameters which were selected are groove angle and preheat temperature at brass side, and welding current. The groove is made only at brass side to compensate the difference in thermal conductivity of brass and SS. The design of experiment was done using Taguchi method for process optimization. Experiments were conducted with different levels of welding parameters and sound weld were created.

The microstructural analyses of the weldment were carried out at the cross section. The microstructure of Brass/J4 stainless steel weldment was investigated using Optical Microscopy. Depth of penetration on stainless steel side is taken as the objective function for Taguchi analysis. The Analysis of Variance (ANOVA) of the response data were also done by Regression analysis on MINITAB software.

Key Words: Dissimilar Welding, gas tungsten arc welding, Taguchi method, Stainless steel, Brass

1. INTRODUCTION

Dissimilar metal welding is the joining of two different alloy systems which have different properties and composition. For dissimilar metal welding, more process parameters and welding constrains are to be taken into consideration than for a conventional, similar metal welding processes since the chemical composition of the base metal alloys and the filler metals are different. Dissimilar metal welds are commonly used in different industries such as power generation, chemical industries, electronics and nuclear industries, to combine different properties of these materials in a single integrated structure. Dissimilar metal welds encountered in power and process industries are most often fusion weld made by more common welding processes [1].

Welding of Stainless Steel and Copper is important because of their increasing applications in industries. The composite structure of stainless steel and copper alloys, composed of dissimilar metals, presents the significant advantage of combining the good mechanical property and corrosion resistance of stainless steel with the good heat conductivity of the copper alloys. This combination of stainless steel and copper alloys is found in pressure vessels, boilers, and other high temperature components. However, welding of stainless steel and copper presents a series of problems. Differences in the physical properties of the two metals, including the thermal conductivity, melting point and thermal expansion, make defect-free dissimilar welding difficult. Stainless steels have low thermal conductivity in comparison to copper and its alloys. Joining of copper to stainless steel can increase the heat dissipation from these alloys during high temperature applications. Copper can be welded with stainless steel by fusion and non-fusion welding processes.

This work focusses on the feasibility of welding of Austenitic Stainless steel J4 and brass C21000 by using Silver-Copper-Zinc alloy named as Silver 40.

2. LITERATURE REVIEW

Magnabosco et al. studied about the gradual continuous concentration variation between the austenite plate and copper is not observed from the center of the weld. But larger concentration variations are observed in the weld. These large local concentration differences and higher cooling rate had control on the microstructure during solidification. Diffusion of copper results in embrittlement of the grain boundaries of austenitic phase and in some cases this caused the formation of micro cracks induced due thermal stresses. The porosity and micro fissures in the joints formed may reduce the ductility of the weld. Further, copper penetrations and micro fissures on the weld could reduce the overall fatigue strength. In particular, thermal fatigue may be very critical because of the thermal instability of the microstructure [2].

Ahmet Z. Sahin et al. showed that the width of the heat-affected zone is due to variation of temperature both in the radial and axial directions. Heat conductivity of copper is 10 times faster than steels. In the case of a higher thermal diffusivity, the heat-affected zone is wider than that corresponding to a lower thermal diffusivity region [3].

T. A. Mai et al. showed that there is an extensive porosity at the joint interface which is caused due to a relatively large air gap between the two welded specimens [4].

Shuhai Chena et al. studied that the grains grow remarkably at the HAZ during laser welding. In welding-brazing mode, liquid SS is also frozen by copper in the solid state, which induced the formation of a rough interface between the stainless steel and the copper. In fusion welding process, a number of fine particles and large chunk of weld metal with SS appear at the interface between the fusion belt and the copper, whereas a mass of spherical particles with the copper mixed into the fusion belt is formed inside the fusion zone [5]. However, the past survey does not show a sound weld between Stainless steel and Copper alloys.

O. Kozlova et al. revealed that Ag – Cu alloys system is commonly used for brazing stainless steel worldwide. This alloy system of Ag – Cu causes good wettability and wetting angle at the stainless steel side [6]. This lead to the selection of Silver- Copper filler wire for our welding process

3. EXPERIMENTAL DETAILS

3.1 Material Details

The base materials selected are stainless steel J4 which is an austenitic Stainless steel, commonly used in high temperature applications and Copper alloy C21000 which has excellent ductility and its melting point is about 1085^0 C. The typical chemical compositions of the materials were determined using spectroscopy and the values are shown in tables 1 and 2.

Table-1: Chemical composition of Austenitic Stainless steel J4

Elements	Weight%
C	0.077
Si	0.237
Mn	8.472
P	0.043
N	0.295
Cr	15.88
Mo	0.03
Ni	0.197
Fe	Balance

Table-2: Chemical composition of Copper alloy

Elements	Weight%
Zn	7.363
Sn	0.012
Pb	0.01
Ni	0.11
Fe	0.055
Cu	Balance

Based on the studies done by Sajjad Gholami Shiri et al., the welding of Stainless steel and copper showed best mechanical characteristics when copper filler material was used [7]. Thus we came across Silver 40 filler which is an alloy of silver, copper and zinc. The composition of the filler is in the ratio silver: copper: zinc is 40:30:30.

3.2 Welding Variables Selection

To do the experiment we decided to select a set of welding variables that are favorable for producing a sound weld. To get the desired welding variables the pilot experiments were carried out and the welding variables were selected as shown in table 3.

Table-3: Parameters and Levels

Parameters	Levels		
	1	2	3
Groove angle	30°	45°	60°
Current(A)	80	100	110
Preheat Temperature(°C)	450	500	600

3.3 Orthogonal Array Selection

In taguchi design of experiment we need to select an orthogonal array for conducting the experiments with minimum number of runs. The selection of orthogonal array can be carried out using two methods: 1) using formula 2) using Array selector.

Selecting an orthogonal array, the minimum number of experiments to be conducted is to be fixed based on the formula below:

N Taguchi = 1+ NV(L – 1)
N Taguchi = Number of experiments to be conducted
NV = Number of parameters
L = Number of levels
In this work, NV = 3 and L = 3.
Hence N Taguchi = 1+ 4 (3-1) = 9

Table-4: Array Selector

	PARAMETERS											
LEVELS		2	3	4	5	6	7	8	9	10	11	12
	2	L4	L4	L8	L8	L8	L8	L12	L12	L12	L12	L16
	3	L9	L9	L9	L18	L18	L18	L18	L27	L27	L27	L27
	4	L16	L16	L16	L16	L32	L32	L32	L32	L32		
	5	L25	L25	L25	L25	L25	L50	L50	L50	L50	L50	L50

We have 3 welding parameters such as groove angle on brass side, preheating temperature of brass and welding current. These three parameters are set to three different values as given in table 3. So we have three parameters with three levels and L9 orthogonal array is selected from the table 4. Hence at least 9 experiments are to be conducted i.e., 9 experimental runs. The L9 orthogonal array is as shown in table 5.

Table-5: Orthogonal Array L9

Experiment Number	Levels		
	A	B	C
1	1	1	1
2	1	2	3
3	1	3	3
4	2	1	2
5	2	2	3
6	2	3	1
7	3	1	3
8	3	2	1
9	3	3	2

Based on this L9 orthogonal array, the experimental design can be tabulated as shown in table 6.

3.4 Experimental Design Using Orthogonal Array L9

Table-6: Experimental Design using L9 orthogonal array

Experiment Number	Levels		
	Groove Angle	Current (A)	Preheat Temperature (°C)
1	30°	80	450
2	30°	100	500
3	30°	110	600
4	45°	80	500
5	45°	100	600
6	45°	110	450
7	60°	80	600
8	60°	100	450
9	60°	110	500

3.5 Joint Configuration

Figures 1 and 2 shows the joint configurations, which is a single bevel joint that we used in this project work. The groove is made only in the copper side to compensate the high thermal conductivity of brass over stainless steel which is almost ten times that of the later.

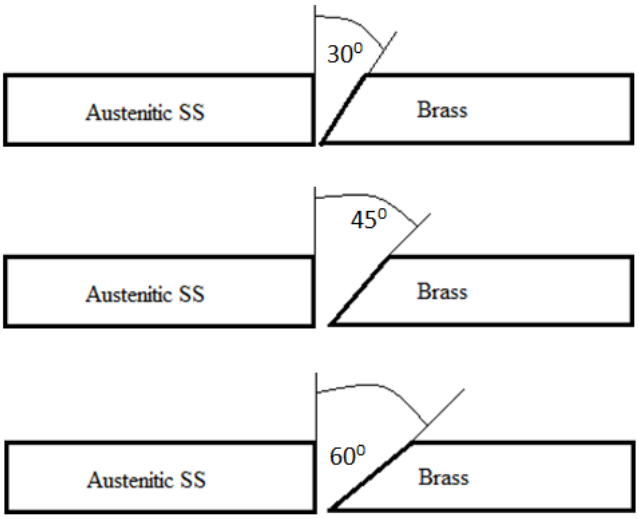

Fig-1: Different bevel joint configurations

3.6 Experiment

The experiments are carried out using the experimental design as we have made. Based on this there should be 9 experimental runs.

First the cutting of the purchased metal sheets of SS and Brass in dimensions of 50mm x 30mm x 3mm is done. Then notch is ground on the Copper alloy specimens. Only Copper specimens need to be grind for making notch since their thermal conductivity is almost 10 times that of the Stainless steel and to compensate this heat dissipation. Keep the Specimens in the configuration as shown in the figure 2. The specimens are to be fixed using fixtures.

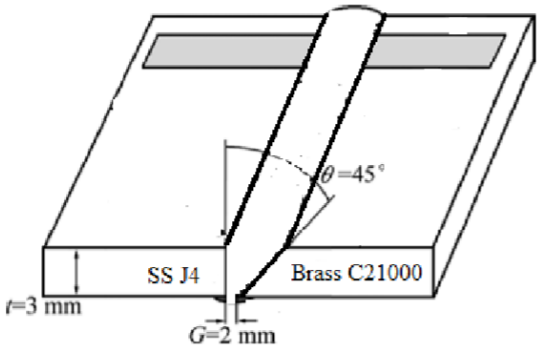

Fig-2: Weld Design

The gap between the sheets should be 2 mm. The specimens are welded together using GTAW technique. Suitable filler

wire of Ag-Cu-Zn alloy i.e.; silver 40 is used. The welding is continued with different welding parameters as per Taguchi Design of Experiment as given in table 6 to obtain a sound weld.

During the conduction of the experiment certain parameters were set to an optimum and they are as follows

3.7 Fixed parameters and welding setup

The Argon gas flow rate was set a flow of 6L/min. The Vertex angle of Tungsten electrode is 60º. The Tungsten electrode diameter is 1.6mm. The size of the cup at the tip of the welding torch is 6mm.

Fig-3: Kemppi Master MLS 2500

Fig-4: Experimental setup

Fig-5: Specimen before welding

4. RESULTS AND DISCUSSIONS

A trail run was carried out on a non-preheated and non-grooved joint and it was a poor weld. During the welding process, initially one of the levels of current was set to be 120 A but, at this current there was excessive melting of the base metal SS J4. Therefore the current was reduced to 110A. Severe distortion was visible in specimen number 3, 4, 5 and 7.

The experiment number 1 with welding parameters of angle 30^0, preheat temperature 450^0C and welding current of 80A was seen to be have serious lack of Fusion and that specimen was eliminated. The microstructures of the remaining specimens were as shown in the following sections.

4.1 Microstructural Analysis

The welded specimens were cut into small samples of size 15 x 15 x 3 mm. Then they were polished for microstructural analysis

The obtained microstructures of the specimens are as shown below:

- Experiment No. 2

Parameters: 30^0 groove angle, 100A current and 500^0C preheat temperature

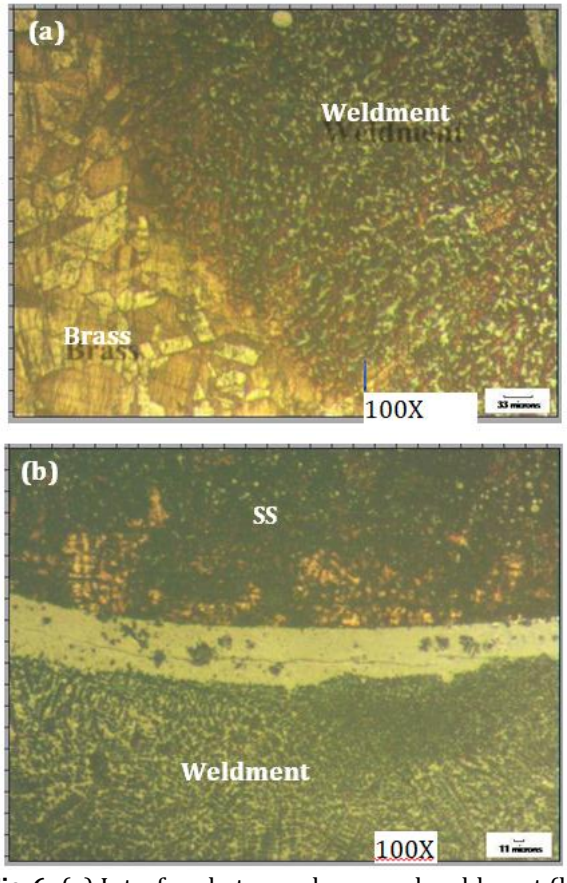

Fig-6: (a) Interface between brass and weldment (b) Interface between weldment and SS

➢ Experiment No. 3

Parameters: 30^0 groove angle, 110A current and 600^0C preheat temperature

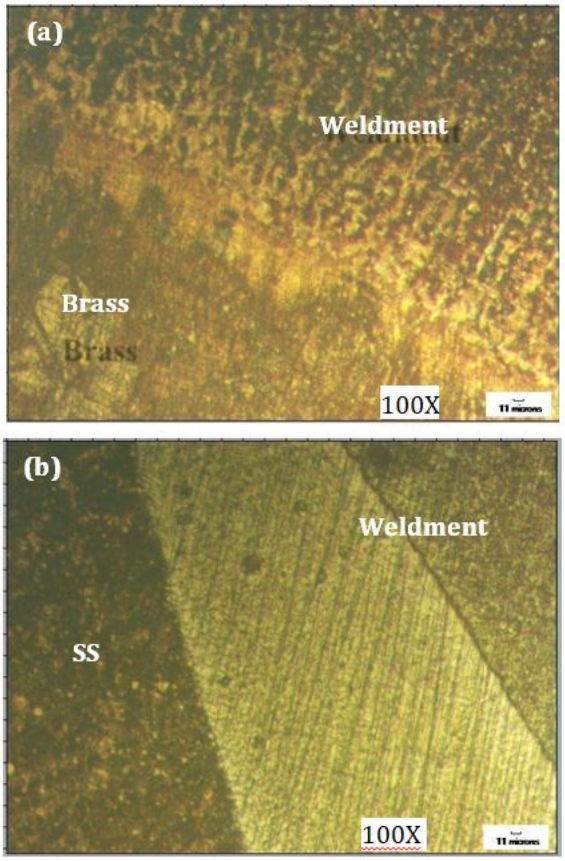

Fig-7: (a) Interface between brass and weldment (b) Interface between weldment and SS

➢ Experiment No. 4

Parameters: 45° groove angle, 80A current and 500^0C preheat temperature

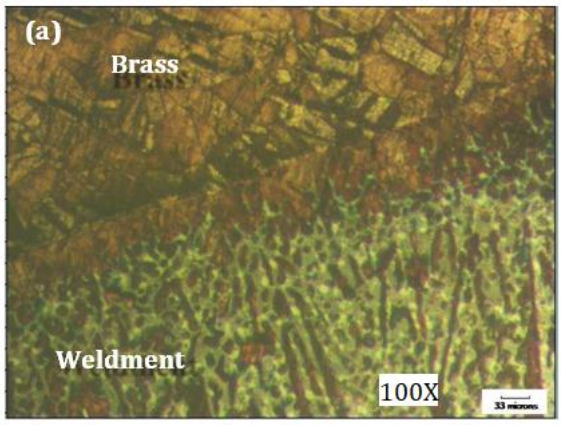

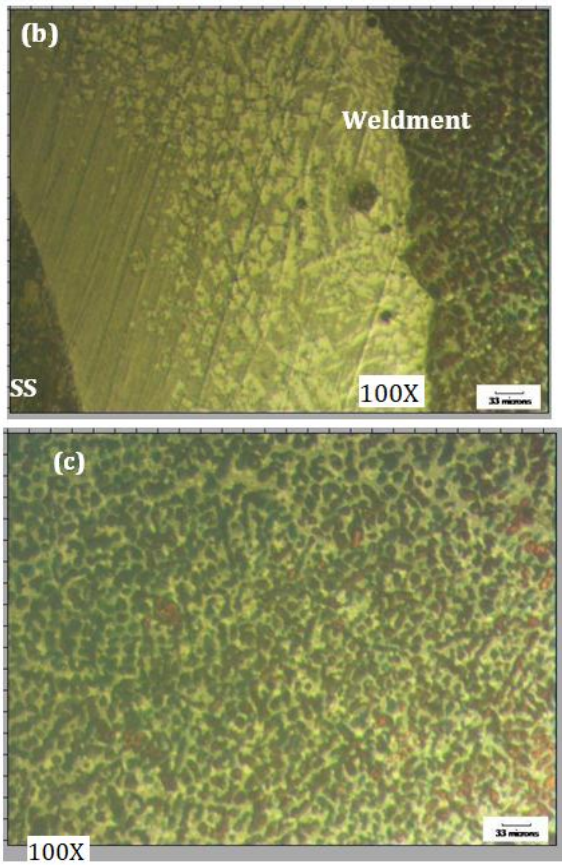

Fig-8: (a) Interface between brass and weldment (b) Interface between weldment and SS (c) Microstructure of weldment

➢ Experiment No. 5

Parameters: 45° groove angle, 100A current and 600^0C preheat temperature

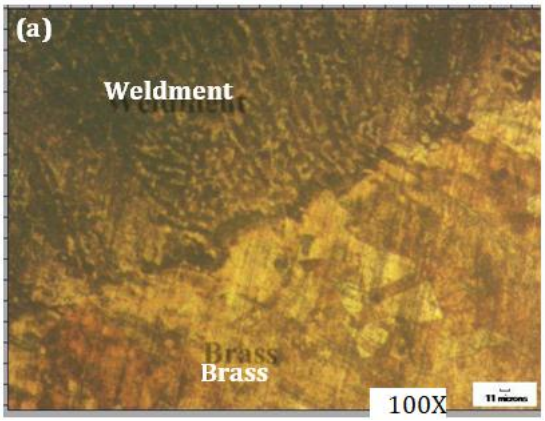

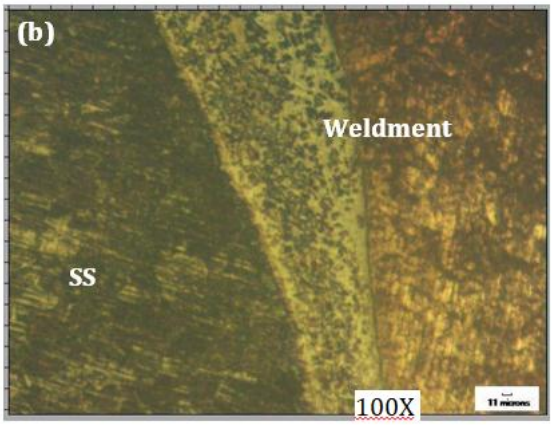

Fig-9: (a) Interface between brass and weldment (b) Interface between weldment and SS

- Experiment No. 6

Parameters: 45° groove angle, 110A current and 450^{0}C preheat temperature

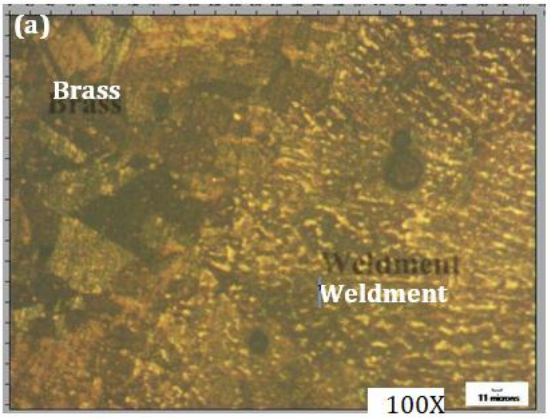

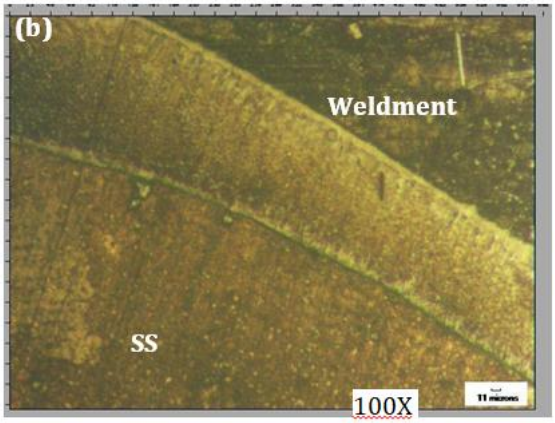

Fig-10: (a) Interface between brass and weldment (b) Interface between weldment and SS

- Experiment No. 7

Parameters: 60°groove angle, 80A current and 600^{0}C preheat temperature

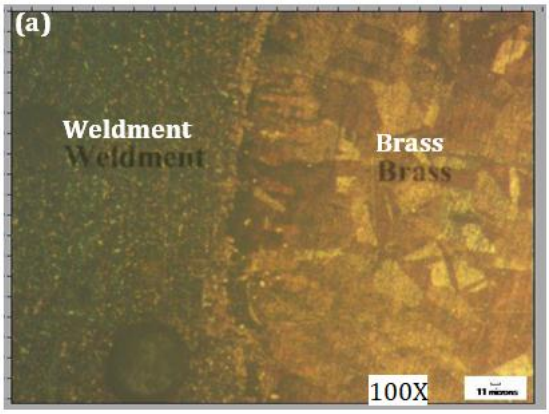

Fig-11: (a) Interface between brass and weldment (b) Interface between weldment and SS

- Experiment No. 8

Parameters: 60° groove angle, 100A current and 450^{0}C preheat temperature

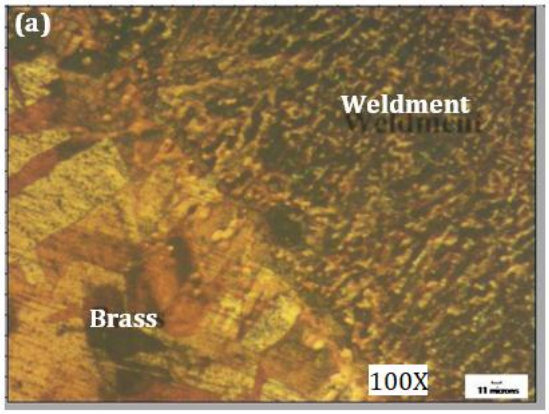

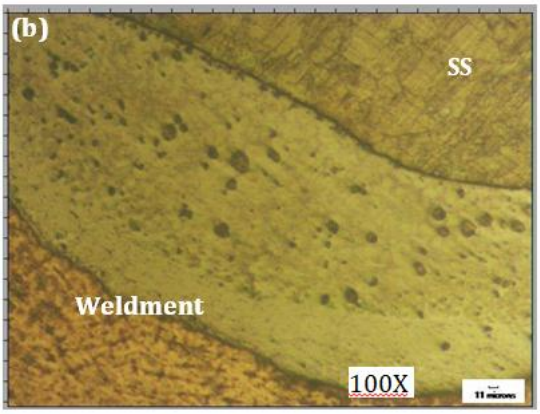

Fig-12: (a) Interface between brass and weldment (b) Interface between weldment and SS

- Experiment No. 9

Parameters: 60° groove angle, 110A current and 500^{0}C preheat temperature

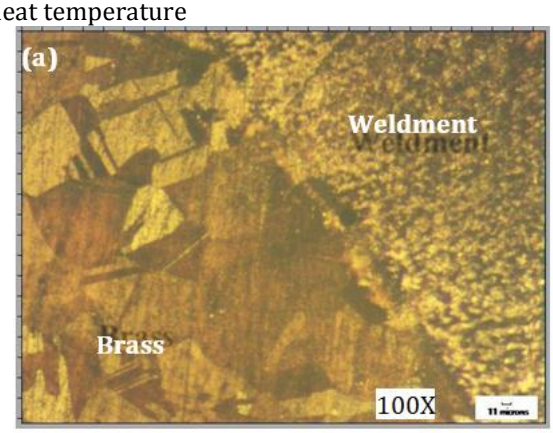

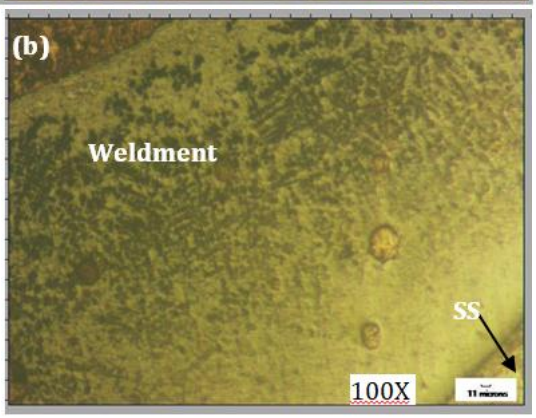

Fig-13: (a) Interface between brass and weldment (b) Interface between weldment and SS

From the microstructures obtained very low amount of porosities were visible in certain cases. From the figures, it is clear that in all experiments the bond between the brass and the filler material is strong enough and sufficient depth of penetration is visible. But in the other side where the bond is between filler material and the stainless steel, the depth of penetration varies in each case. Therefore the strength of the joint depends on the depth on penetration on the stainless steel side and here we analyze the depth of penetration in the following sections.

4.2 Observations

Table-7: Experimental observations

Experiment number	Levels					Heat Input H=(AV×0.06)/s (KJ/mm)
	Groove Angle	Current (A)	Preheat temperature (°C)	Voltage (V)	Time (s)	
1	30°	80	450	8.6	38	32
2	30°	100	500	10.1	35	42. 67
3	30°	110	600	11.5	33	49.93
4	45°	80	500	10.2	32	31.38
5	45°	100	600	11.4	41	56.52
6	45°	110	450	11.2	36	53.56
7	60°	80	600	10.7	43	44.27
8	60°	100	450	11.3	55	74.58
9	60°	110	500	12.7	46	77.61

4.3 Determination of Depth of Penetration

Depth of penetration in each experiment was found out using the image analyzing software IMAGE J. The mean value of the depth of penetration is given in the below table:

Table-8: Depth of penetration in each experiment

Experiment Number	Depth of penetration (microns)
1	No bond
2	113.264
3	327.34
4	438.964
5	111.219
6	184.596
7	453.568
8	294.294
9	616.069

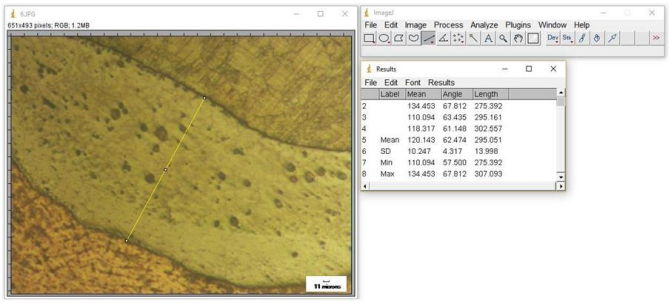

Fig-14: Determination of depth of penetration using IMAGE J

4.4 Taguchi Analysis of Obtained Results

Taguchi analysis was done using MINITAB application software. Response tables for means and S/N ratios were obtained and graphs of the tables were plotted on the software. The factor of consideration for Taguchi analysis is the depth of penetration in the stainless steel side of the weldment.

Table-9: Response table for means

Level	Angle	Current	Preheat temperature
1	146.9	297.5	159.6
2	244.9	172.9	389.4
3	454.6	376	297.4
Delta	307.8	203.1	229.8
Rank	1	3	2

The Response values for the means are as shown in table 9. The differences in the means were maximum for groove angle which is 307.8 and followed by preheat temperature with 229.8 and the current with 203.1. This implies that the effect of groove angle is larger and that of welding current is minimum on the depth of penetration of filler material towards the stainless steel base metal. The plots for means against the main factors such as angle current and preheat temperatures are shown in figure below.

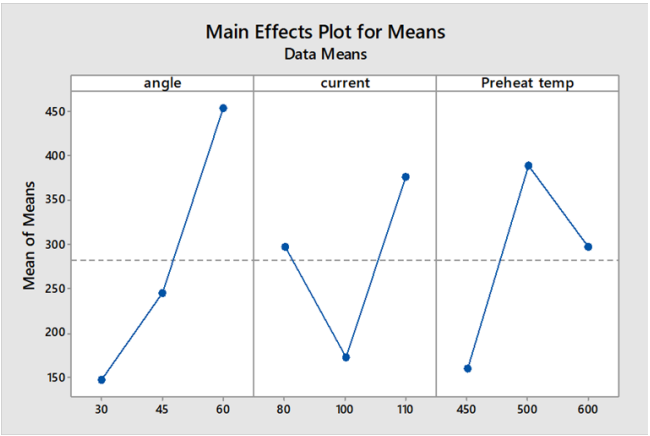

Fig-15: Graphs showing parameter levels v/s mean

In Taguchi's design method the design parameters (factors that can be controlled by designers) and noise factors (factors that cannot be controlled by designers, such as environmental factors) are considered influential on the product quality. The Signal to Noise (S/N) ratio is used in this analysis which takes both the mean and the variability of the experimental result into account. In the present study the characteristic chosen is depth of penetration and higher-the-better performance is taken into consideration.

The Response values for the S/N ratios are as shown in table 10. The difference in the means of S/N ratios was maximum for groove angle which is 22.31 and followed by preheat temperature with 18.34 and the current with 15.15.

Table-10: Response values for the S/N ratio

Level	Angle	Current	Preheat Temperature
1	30.46	35.33	31.57
2	46.37	43.79	49.91
3	52.77	50.47	48.12
Delta	22.31	15.15	18.34
Rank	1	3	2

The values of S/N ratios for each experiment are shown in table 11. The effect of S/N ratios against the main parameters – Groove angle, Current, Preheat temperature- are plotted in figure 16.

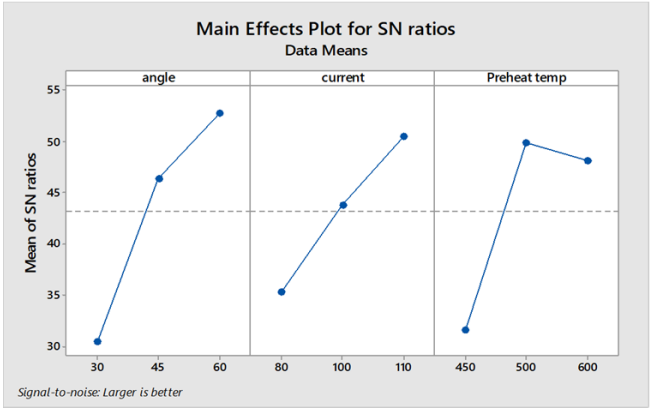

Fig-16: Graphs showing parameter levels versus S/N Ratios

Table-11: S/N ratios for each experiment

Experiment number	Angle	Current (A)	Preheat temperature (^{0}C)	Depth of Penetration (microns)	S/N Ratio
1	30^0	80	450	_	0
2	30^0	100	500	113.264	41.08184

3	30^0	110	600	327.34	50.29998
4	45^0	80	500	438.964	52.84858
5	45^0	100	600	111.219	40.92358
6	45^0	110	450	184.596	45.32445
7	60^0	80	600	453.568	53.13285
8	60^0	100	450	294.294	49.37563
9	60^0	110	500	616.069	55.79259

It is evident from the graph that the Signal to Noise ratio is maximum when the parameters are groove angle 60^0, Welding current 110 A and Preheat temperature 500^0C. When we cross check this value with values for depth of penetration of the weldment it is clear that the specimen with the same exact value of higher S/N ratio showed the maximum depth of penetration of 616 microns.

Therefore the optimum values of the parameters for obtaining maximum depth of penetration is with parameters of groove angle 60^0, Welding current 110 A and Preheat temperature 500^0C.

4.4.1 Regression Analysis: Depth of Penetration versus angle, current, Preheat temperature

Analysis of Variance Approach is applied to find the considerable factors. This ANOVA is done using MINITAB 17 application software. The result of the analysis is as shownin the following table.

Table-12: Analysis of Variance for depth of penetration

Source	DF	Adj SS	Adj MS	F-Value	P-Value
Regression	3	159255	53085	1.72	0.279
angle	1	141781	141781	4.58	0.085
current	1	2517	2517	0.08	0.787
Preheat temperature	1	14957	14957	0.48	0.518
Error	5	154714	30943		
Total	8	313968			

4.4.2 Development of Mathematical modelling

The function that represents the response for depth of penetration can be expressed mathematically as DOP = f (Angle(A), Current(C), Preheat temperature(T)) and the relationship is shown as a multiple regression model. The general form of a mathematical regression model is as shown below

Depth of penetration = $a0 + a1A + a2C + a3T + a11A^2 + a22C^2 + a33T^2 + a12AC + a13AT + a23CT$ **(Equation-1)**

Different regression models were fitted to the above data and the coefficients values (ai) are calculated using least squares method on MINITAB software.

4.4.3 Regression Model

By neglecting insignificant factors on depth of penetration of weld using regression analysis and ANOVA final model was developed as shown below:

Depth of penetration = -646 + 10.25A + 1.34C + 0.654T

(Equation-2)

Regression coefficient is shown in the table below from the analysis done on MINITAB 17.

Table-13: The coefficient of regression model

Term	Coefficient	SE Coefficient	T-Value	P-Value
Constant	-646	702	-0.92	0.399
Angle	10.25	4.79	2.14	0.085
Current	1.34	4.7	0.29	0.787
Preheat temperature	0.654	0.94	0.7	0.518

Based on the regression model formed the best values for the particular parameter can be determined by substituting different parameter values in equation 2. The resulting values obtained by substituting parameter levels are shown in table 14. The errors between the practical values and the theoretical regression model are also depicted in the table.

Table-14: Results of Regression analysis

Experiment no.	Angle	Current (A)	Preheat temp (°C)	DOP-Practical (microns)	DOP-Regression Analysis	Error
1	30^0	80	450	–	–	–
2	30^0	100	500	113.264	122.5	-9.236
3	30^0	110	600	327.34	201.3	126.04
4	45^0	80	500	438.964	249.45	189.514
5	45^0	100	600	111.219	341	-229.781
6	45^0	110	450	184.596	256.95	-72.354

7	60^0	80	600	453.568	468.6	-15.032
8	60^0	100	450	294.294	397.3	-103.006
9	60^0	110	500	616.069	443.4	172.669

The errors shown up indicate that there are several noise factors that significantly affects the quality of the weld. This noise factors may be environmental, machine errors and human errors.

In practical assessment maximum depth of penetration was shown by experiment number 9 with welding angle 60^0, Current 110 A and Preheat temperature 500^0C. But as per the values of regression analysis done, maximum depth of penetration can be obtained in experiment number 7 with welding angle 60^0, Current 80A and Preheat temperature 600^0C. The confirmation experiments are to be done to verify these errors.

5. CONCLUSIONS

The GTAW welding of Brass and Austenitic Stainless steel is studied with microstructural analysis and statistical analysis using Taguchi method for the process optimization, and the following conclusions were obtained:

i. Sound weld is obtained between austenitic Stainless steel grade J4 and brass grade C21000 using special filler wire, Silver 40 with a typical composition of 40% Ag, 30% Cu and 30% Zn.

ii. The design of the welding process was done using Taguchi design of Experiment, thus the number of experiments were reduced from 27 to 9 optimised sets.

iii. Various parameters such as groove angle, welding current and preheat temperature were selected as process parameters for the statistical experiments.

iv. Microstructures were obtained using optical microscope at the cross section of each weldment. Metallography of weld zone, steel section and brass section were obtained.

v. Depth of penetration obtained after welding at the stainless steel side was measured using image J software and was taken as Response data for statistical analysis.

vi. The response table for the mean of mean values of depth of penetration and the S/N ratios were tabulated and graphs were plotted using MINITAB software

vii. From the experiments, the optimised weld was obtained with welding parameters of groove angle 60^0, Preheat temperature 500^0 C and welding current of 110 A as it showed the maximum depth of penetration of 616 microns and gives maximum S/N ratio during the analysis.

viii. The Regression analysis of the response were carried out using Analysis of Variance (ANOVA) and a better result of depth of penetration was shown for experiment with groove angle 60^0, Preheat temperature 600^0 C and welding current of 80 A.

ix. The optimised values of parameters obtained by analysis of practical response and regression method showed differences and this variation is due to the noise factors which affected the welding process

REFERENCES

[1] Carlone, P. and Astarita, A., 2019. Dissimilar Metal Welding

[2] Magnabosco, I., Ferro, P., Bonollo, F. and Arnberg, L., 2006. An investigation of fusion zone microstructures in electron beam welding of copper–stainless steel. Materials Science and Engineering: A, 424(1-2), pp.163-173

[3] Sahin, A.Z., Yibas, B.S., Ahmed, M. and Nickel, I., 1998. Analysis of the friction welding process in relation to the welding of copper and steel bars. Journal of Materials Processing Technology, 82(1-3), pp.127-136

[4] Mai, T.A. and Spowage, A.C., 2004. Characterization of dissimilar joints in laser welding of steel–kovar, copper–steel and copper–aluminium. Materials Science and Engineering: A, 374(1-2), pp.224-233

[5] Chen, S., Huang, J., Xia, J., Zhao, X. and Lin, S., 2015. Influence of processing parameters on the characteristics of stainless steel/copper laser welding. Journal of Materials Processing Technology, 222, pp.43-51

[6] Kozlova, O., Voytovych, R., Devismes, M.F. and Eustathopoulos, N., 2008. Wetting and brazing of stainless steels by copper–silver eutectic. Materials Science and Engineering: A, 495(1-2), pp.96-101.

[7] Shiri, S.G., Nazarzadeh, M., Sharifitabar, M. and Afarani, M.S., 2012. Gas tungsten arc welding of CP-copper to 304 stainless steel using different filler materials. Transactions of Nonferrous Metals Society of China, 22(12), pp.2937-2942.